 Communications in Theoretical Physics

Commun. Theor. Phys. 74 (2022) 125001 (8pp) https://doi.org/10.1088/1572-9494/ac8afd

Effect of near $\mathcal{PT}$-symmetric potentials on nonlinear modes for higher-order generalized Ginzburg–Landau model

Da Lin, Kai-Ru Dong, Jia-Rui Zhang and Yu-Jia Shen*

College of Science, China Agricultural University, Beijing 100083, China

E-mail: yjshen2018@cau.edu.cn

Received 10 July 2022, revised 8 August 2022
Accepted for publication 19 August 2022
Published 21 November 2022

Abstract

In this paper, we study the higher-order generalized Ginzburg–Landau model which contributes to describing the propagation of optical solitons in fibers. By means of the Hirota bilinear method, the analytical solutions are obtained and the effect of relevant parameters is analyzed. Modulated by the near parity-time-symmetric potentials, the nonlinear modes with 5% initial random noise are numerically simulated to possess stable evolution. Furthermore, the evolution of nonlinear modes is displayed through the adiabatical change of some parameters. The investigation of the present work is intended as a contribution to the work for the higher-order generalized Ginzburg–Landau model.

Supplementary material for this article is available online

Keywords: generalized Ginzburg–Landau model, parity-time symmetry, stability of soliton solutions

(Some figures may appear in colour only in the online journal)

1. Introduction

Optical solitons, which have the unique characteristic that waveform and velocity remain unchanged over long distant propagation, have been paid increasing attention in recent years [1–5]. It is found that the formation mechanism of optical solitons during the propagation process is the balance between group velocity dispersion and the self-phase modulation effect in the anomalous dispersion region [1]. To describe the propagation of optical solitons in optical fibers, the nonlinear Schrödinger equation (NLSE) known as an important and universal model has been developed with some generalizations and soliton solutions presented [6–13]. Nevertheless, the generalized Ginzburg–Landau equation (GGLE), which is widely applied in such fields as superconductivity, liquid crystal, Bose–Einstein condensate, can be considered as a dissipative generalization of NLSE [14–17]. Different analytical and numerical methods have been applied to the GGLE, while various novel solutions including the pulsating, erupting and creeping solitons have been obtained [18–23]. By means of numerical simulations, the stability of various solutions has been proved [24, 25]. For a wider application prospect, the model has been extended to higher-dimension and higher-order cases [26–30]. Moreover, parity-time ($\mathcal{PT}$) symmetric potentials have been introduced to the GGLE with several interesting results [25, 31, 32]. Though different $\mathcal{PT}$-symmetric behaviors have been studied theoretically or observed in experiments [33–38], limited research has been done which is relevant to the higher-order GGLE. In previous work, we have investigated the fourth-order GGLE with quintic nonlinearities and near $\mathcal{PT}$-symmetric structures [39].

In this paper, we will study the GGLE with third-order dispersion and nonlinear gradient:

$$\begin{aligned} &\mathrm{i}u_t + \alpha(x)u_{xx} + U(x,t)u + \beta(x,t)|u|^2u \\ &+ \mathrm{i}\sigma(t)u_{xxx} + \mathrm{i}\gamma(t)|u|^2u_x + \mathrm{i}\rho(t)u_x = 0, \end{aligned} \tag{1}$$

where $u(x, t)$ represents a complex wave envelope, x denotes the propagation distance and t is the time. The subscripts denote the partial derivative with respect to x or t and i

* Author to whom any correspondence should be addressed.

represents the imaginary unit. $\alpha(x)$, $U(x, t)$ and $\beta(x, t)$ are complex functions that can be assumed as $\alpha=\alpha_1+\mathrm{i}\alpha_2$, $U=V+\mathrm{i}W$, $\beta=\beta_1+\mathrm{i}\beta_2$. $\alpha(x)$, $U(x, t)$, $\beta(x, t)$, $\sigma(t)$ and $\gamma(t)$ can describe the variable effect of group velocity dispersion, gain or loss, self-phase modulation, third-order dispersion and nonlinear gradient terms, respectively [18, 25, 30, 40].

There are three special cases that can be reduced by equation (1).

(1) When $\alpha_2(x)=W(x, t)=\beta_2(x, t)=0$, equation (1) turns into the third-order NLSE. It has been used to describe the propagation of ultra-short pulses and optical solitons in fibers in [6, 7, 41]. Some exact solutions and the corresponding abundant structures have been obtained [7], and the linear stability of solitons has been studied [6].
(2) When $\sigma(t)=\gamma(t)=\rho(t)=0$, equation (1) can be reduced to the second-order GGLE. The analytical solutions have been derived by means of the Hirota bilinear method [21, 25, 42, 43]. The stability of soliton has been analyzed via numerical simulations in [25, 42].
(3) When $\sigma(t)=\gamma(t)=\rho(t)=0$ and $U(x, t)$ is $\mathcal{PT}$-symmetric. Equation (1) is changed into the GGLE with $\mathcal{PT}$-symmetric potential, which has been less investigated so far except [25]. The effect of near $\mathcal{PT}$-symmetric potentials on nonlinear modes has been reported [32].

The rest of this paper is arranged as follows. In section 2, the bilinear form of equation (1) is derived under some constraints. In addition, soliton solutions of equation (1) with constant and variable coefficients are obtained respectively. In section 3, the stable transmission of nonlinear modes is verified through numerical simulations with 5% perturbations. The effect of near $\mathcal{PT}$-symmetric potentials is discussed with relevant figures illustrated, and the adiabatic change of some parameters is considered. Finally, the conclusions are given in section 4.

2. Analytical solutions of equation (1)

The analytical solutions of equation (1) are derived by the Hirota bilinear method. Through variable transformation

$$u(x, t)=\frac{G(x, t)}{F(x, t)}, \tag{2}$$

with the real function F and complex G, and the constraint $\alpha\gamma=3\sigma\beta$, the bilinear equations of equation (1) are written as

$$\begin{aligned}[\mathrm{i}D_t+\alpha D_x^2+U+\mathrm{i}\sigma D_x^3+\mathrm{i}\rho D_x]G\cdot F&=0,\\ \alpha D_x^2F\cdot F-\beta|G|^2&=0.\end{aligned} \tag{3}$$

The Hirota operator is defined by [44]

$$D_x^mD_t^nG(x, t)\cdot F(x, t)=\frac{\partial^m}{\partial y^m}\times\frac{\partial^n}{\partial s^n}G(x+y, t+s)F(x-y, t-s)|_{y=0,s=0}. \tag{4}$$

We expand G and F in power series of ϵ as

$$\begin{aligned}G&=\epsilon G_1+\epsilon^3G_3+\epsilon^5G_5+\cdots,\\ F&=1+\epsilon^2F_2+\epsilon^4F_4+\epsilon^6F_6+\cdots,\end{aligned} \tag{5}$$

where ϵ is a small parameter, $G_i(i=1, 3, 5, \ldots)$ and $F_j(j=2, 4, 6, \ldots)$ are functions of x and t to be determined.

In this section, we study two cases of constant and variable coefficients. For the sake of calculation, we set $\epsilon=1$. The analytical expression of a single soliton solution for equation (1) is

$$u(x, t)=\frac{G_1}{1+F_2}. \tag{6}$$

Case 1:

Under the constraints $\beta_1=c_0\alpha_1$, $\beta_2=c_0\alpha_2$, $W=-k_1^2\alpha_2$, where $\alpha_i(i=1, 2)$, c_0, k_1 are real constants, we substitute equation (5) into equation (3) and collect the coefficients of ϵ with the same power. Then we can get

$$\begin{aligned}G_1(x, t)&=(m_1+\mathrm{i}m_2)\mathrm{e}^{k_1x+(w_1+\mathrm{i}w_2)t},\\ F_2(x, t)&=A_1\mathrm{e}^{2k_1x+2w_1t},\\ w_1&=-k_1\rho-k_1^3\sigma,\\ w_2&=V+k_1^2\alpha_1,\\ A_1&=\frac{c_0(m_1^2+m_2^2)}{8k_1^2},\end{aligned} \tag{7}$$

i.e. the soliton solution of equation (1) with constant coefficients, where m_i, $w_i(i=1, 2)$, ρ, σ, V, W are real constants.

Case 2:

Similarly, we set $\beta_1(x, t)=2c_0(t)\alpha_1(x)$, $\beta_2(x, t)=2c_0(t)\alpha_2(x)$, $c_0(t)=c_1\mathrm{e}^{\int 2W_1(t)\,\mathrm{d}t}$, $V(x, t)=-k_1^2\alpha_1(x)+V_1(t)$, $W(x, t)=-k_1^2\alpha_2(x)+W_1(t)$ and derive

$$\begin{aligned}G_1(x, t)&=(m_1+\mathrm{i}m_2)A_1(t)\mathrm{e}^{k_1x+w_1(t)+\mathrm{i}w_2(t)},\\ F_2(x, t)&=\frac{m_1^2+m_2^2}{4k_1^2}\mathrm{e}^{2k_1x+2w_1(t)},\\ A_1(t)&=\mathrm{e}^{\int -W_1(t)\,\mathrm{d}t},\\ w_1(t)&=\int[-k_1\rho(t)-k_1^3\sigma(t)]\,\mathrm{d}t,\\ w_2(t)&=\int V_1(t)\,\mathrm{d}t,\end{aligned} \tag{8}$$

where m_i $(i=1, 2)$, k_1 are real constants. Substituting Expressions (8) into (6), we get the analytical soliton solution likewise.

By modulating dispersion and gain or loss terms, we illustrate their effect of them on the structure and propagation of soliton in figure 1. In figure 1(a), when σ, ρ and $W_1(t)$ are chosen as sine functions, the amplitude of the soliton varies with time periodically. Once the dispersion terms are taken as aperiodic functions like exponential functions, the amplitude is still periodic except for a phase shift around $t=0$. Obviously, the periodicity of amplitude is only related to the gain or loss term and the dispersion terms affect the structures. As shown in figure 1(c), the value of k_1 is adjusted. When the value of k_1 reduces to 0.5, the maximum amplitude decreases and the structure of soliton has changed.

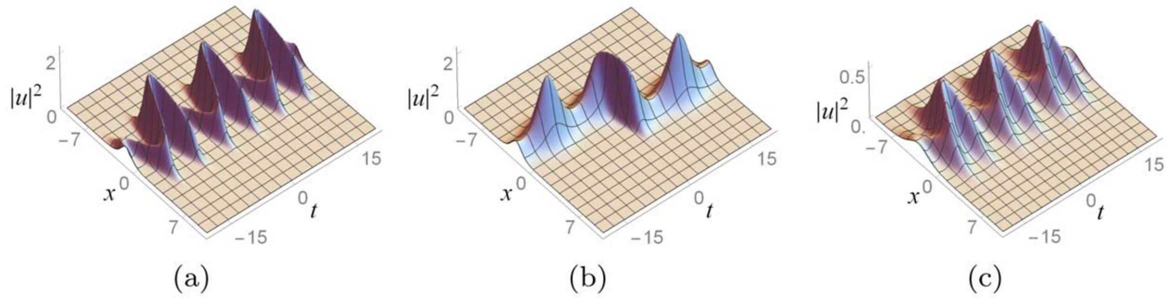

Figure 1. Structures of soliton solution with variable coefficients. Parameters are chosen as: (a) $W_1(t) = 0.2\sin(0.5t)$, $\rho(t) = \sigma(t) = \sin t$, (b) $W_1(t) = 0.2\sin(0.5t)$, $\rho(t) = \sigma(t) = e^{-t^2}$, (c) $W_1(t) = 0.2\sin(0.5t)$, $\rho(t) = \sigma(t) = \sin t$, $k_1 = 0.5$ and other parameters are fixed as 1.

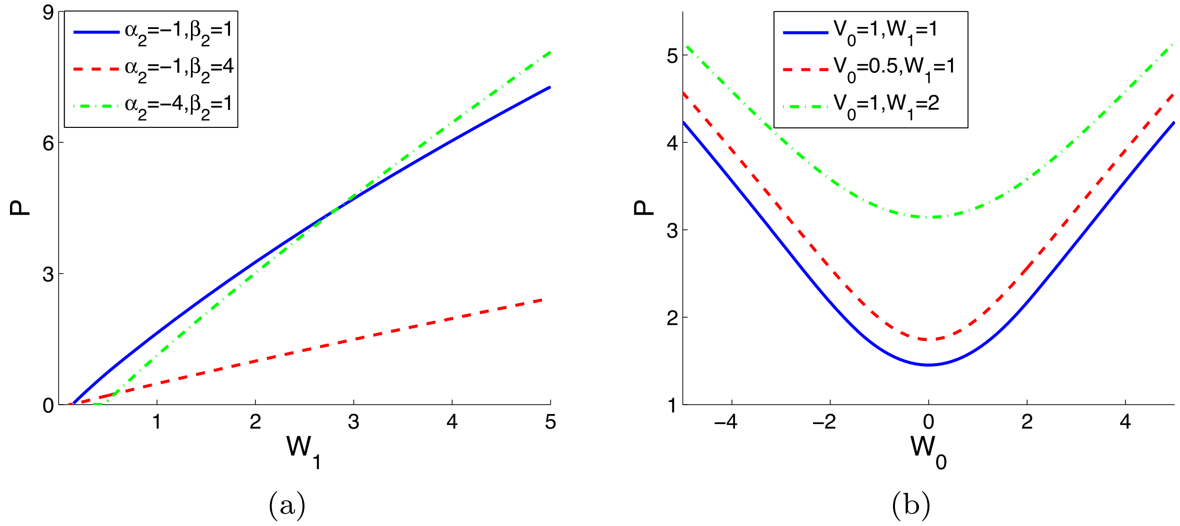

Figure 2. Effect of parameters on the power of nonlinear modes under near $\mathcal{PT}$-symmetric Scarf-II potential. (a) $\alpha_1 = \beta_1 = V_0 = W_0 = 1$, (b) $\alpha_1 = \beta_1 = \beta_2 = 1$ and $\alpha_2 = -1$.

3. Numerical simulations of equation (1)

The stability of solitary wave solutions plays a crucial role in practical applications. Due to the non-integrability of equation (1), the stability of solitary waves propagating in non-Kerr nonlinear media can not be guaranteed [9]. So the stability will be tested in this section via numerical simulations with a perturbation of 5% initial random noise. Furthermore, the modified squared-operator and pseudospectral methods are used in the numerical simulations [45]. Under near $\mathcal{PT}$-symmetric potential, the equation (1) can be rewritten as

$$\begin{aligned} &\mathrm{i}u_t + (\alpha_1 + \mathrm{i}\alpha_2)u_{xx} + [V(x) + \mathrm{i}W(x)]u \\ &+(\beta_1 + \mathrm{i}\beta_2)|u|^2u + \mathrm{i}\sigma u_{xxx} \\ &+ \mathrm{i}\gamma|u|^2u_x + \mathrm{i}\rho u_x = 0, \end{aligned} \tag{9}$$

where σ, γ, ρ, α_i, β_i $(i = 1, 2)$ are real constants and $V + \mathrm{i}W$ denotes the near $\mathcal{PT}$-symmetric potential.

The nonlinear mode of equation (9) can be defined as

$$u(x, t) = \phi(x)e^{-\mathrm{i}\mu t}, \tag{10}$$

where μ is a real propagation constant. We will first study the stability of nonlinear modes with the effect of the last three terms ignored, and reduce equation (9) to the second-order GGLE:

$$\begin{aligned} &\mathrm{i}u_t + (\alpha_1 + \mathrm{i}\alpha_2)u_{xx} + [V(x) \\ &+ \mathrm{i}W(x)]u + (\beta_1 + \mathrm{i}\beta_2)|u|^2u = 0. \end{aligned} \tag{11}$$

In the last subsection, these parameters will be considered again through adiabatical excitation of them.

3.1. Nonlinear modes under near $\mathcal{PT}$-symmetric Scarf-II potential

We introduce the near $\mathcal{PT}$-symmetric Scarf-II potential [32]

$$\begin{aligned} &V(x) = V_0\,\mathrm{sech}^2(x), \\ &W(x) = W_0\,\mathrm{sech}(x)\tanh(x) - W_1\,\mathrm{sech}^2(x), \end{aligned} \tag{12}$$

where the value of real constants V_0, W_0 and W_1 can be modulated to obtain stable nonlinear modes.

The power of nonlinear mode is defined as $P = \int_{-\infty}^{+\infty} |\phi(x, t)|^2\, dx$. Figure 2(a) shows the result that stable evolution does not exist when the value of W_1 approaches zero because the potential turns into $\mathcal{PT}$-symmetric Scarf-II potential. The power decreases obviously with increasing the value of β_2, but α_2 has less effect on the power. The two curves with different values of α_2 intersect at $W_1 = 2.8$.

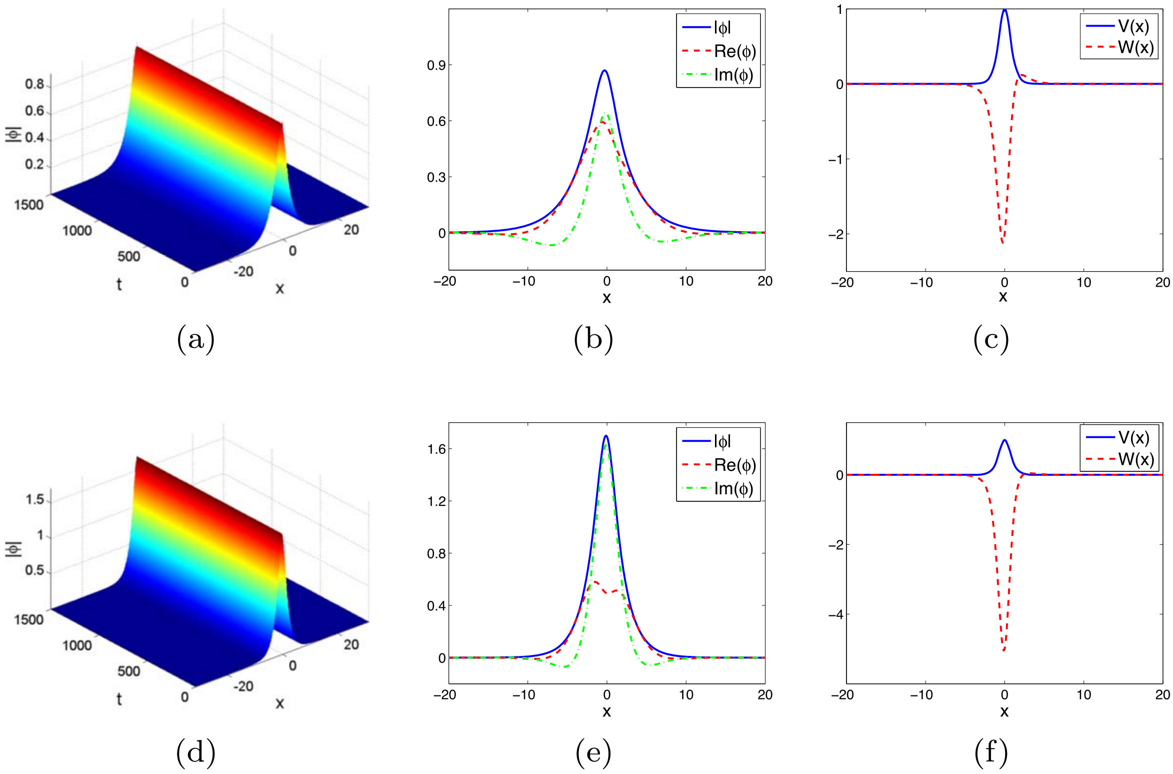

Figure 3. Stable evolution of nonlinear modes under near $\mathcal{PT}$-symmetric Scarf-II potential. (a), (b), (c) $W_1=2$, (d), (e), (f) $W_1=5$. $\alpha_2=-4$ and other parameters are fixed as 1.

Symmetric curves with respect to $W_0=0$ are shown in figure 2(b). Moreover, they attain the lowest power at the point $W_0=0$ simultaneously. By the change of V_0 or W_1, the lowest power can be adjusted.

The stable nonlinear modes under near $\mathcal{PT}$-symmetric Scarf-II potential are shown in figures 3(a) and 3(d) with 5% initial perturbations. Increasing the value of W_1 to 5, the amplitude becomes larger and the nonlinear mode has a narrower width. That is to say, the energy becomes more concentrated than before. At the same time, the imaginary part of the nonlinear mode takes up a larger proportion.

3.2. Nonlinear modes under near $\mathcal{PT}$-symmetric δ-signum potential

Equation (11) with near $\mathcal{PT}$-symmetric δ-signum potential is discussed as follows. The potential can be expressed as

$$\begin{aligned} V(x) &= 2V_0\delta(x),\\ W(x) &= W_0\mathrm{sign}(x)\mathrm{e}^{-V_0|x|} - W_1\delta(x), \end{aligned} \tag{13}$$

where $\delta(x)=\lim_{a\to 0^+} g(x;a)$, $g(x;a)=\frac{\mathrm{e}^{-x^2/a^2}}{a\sqrt{\pi}}$, and a is set as 0.01 for calculation expediently [46]. It is found that the two curves with different values of α_2 are nearly parallel to each other in figure 4(a). Figure 4(b) illustrates the effect of near $\mathcal{PT}$-symmetric δ-signum potential. When $V_0=0.4$, the nonlinear modes exist even if $W_1=0$. At the points in blue solid and red dashed curves, the potential reduces to $\mathcal{PT}$-symmetric δ-signum potential, which satisfies that $V(x)=V(-x)$ and $W(-x)=-W(x)$.

Next, we consider the evolution of nonlinear modes with the potential. In the numerical simulations, 5% initial random noise is added likewise. Figures 5(a), (d) and (g) show the stable evolution of peakons, while W_0 affects the amplitude and period of oscillation. In contrast to figure 5(a), the peakon maintains a certain value and does not oscillate when the value of V_0 increases to 1 in figure 5(g).

3.3. Adiabatic excitation and evolution of the nonlinear modes

The adiabatic change of parameters in equation (9) with near $\mathcal{PT}$-symmetric Scarf-II potential will be considered. The 'switch-on' function in [47] is used so that the parameters can be smoothly adjusted:

$$\xi(t)=\begin{cases}\xi^{(\mathrm{ini})}, & t=0,\\ \xi^{(\mathrm{ini})}+\dfrac{\xi^{(\mathrm{end})}-\xi^{(\mathrm{ini})}}{2}\left[1+\sin\left(\dfrac{\pi}{500}t-\dfrac{\pi}{2}\right)\right], & 0<t<500,\\ \xi^{(\mathrm{end})}, & 500\leqslant t\leqslant 1500.\end{cases} \tag{14}$$

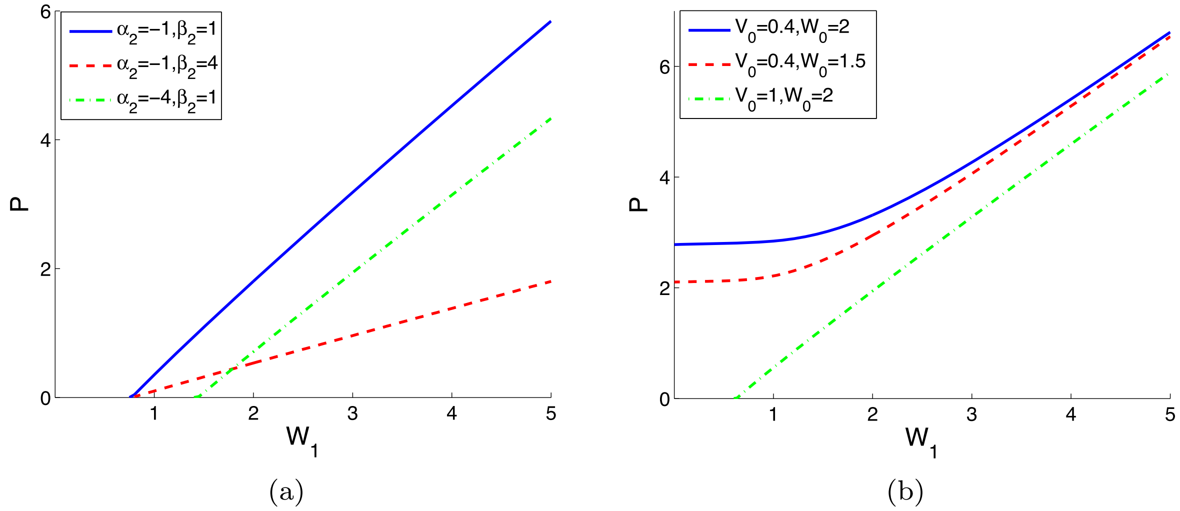

Figure 4. Effect of parameters on the power of nonlinear modes under near $\mathcal{PT}$-symmetric δ-signum potential. (a) $\alpha_1 = \beta_1 = V_0 = W_0 = 1$, (b) $\alpha_1 = \beta_1 = \beta_2 = 1$ and $\alpha_2 = -1$.

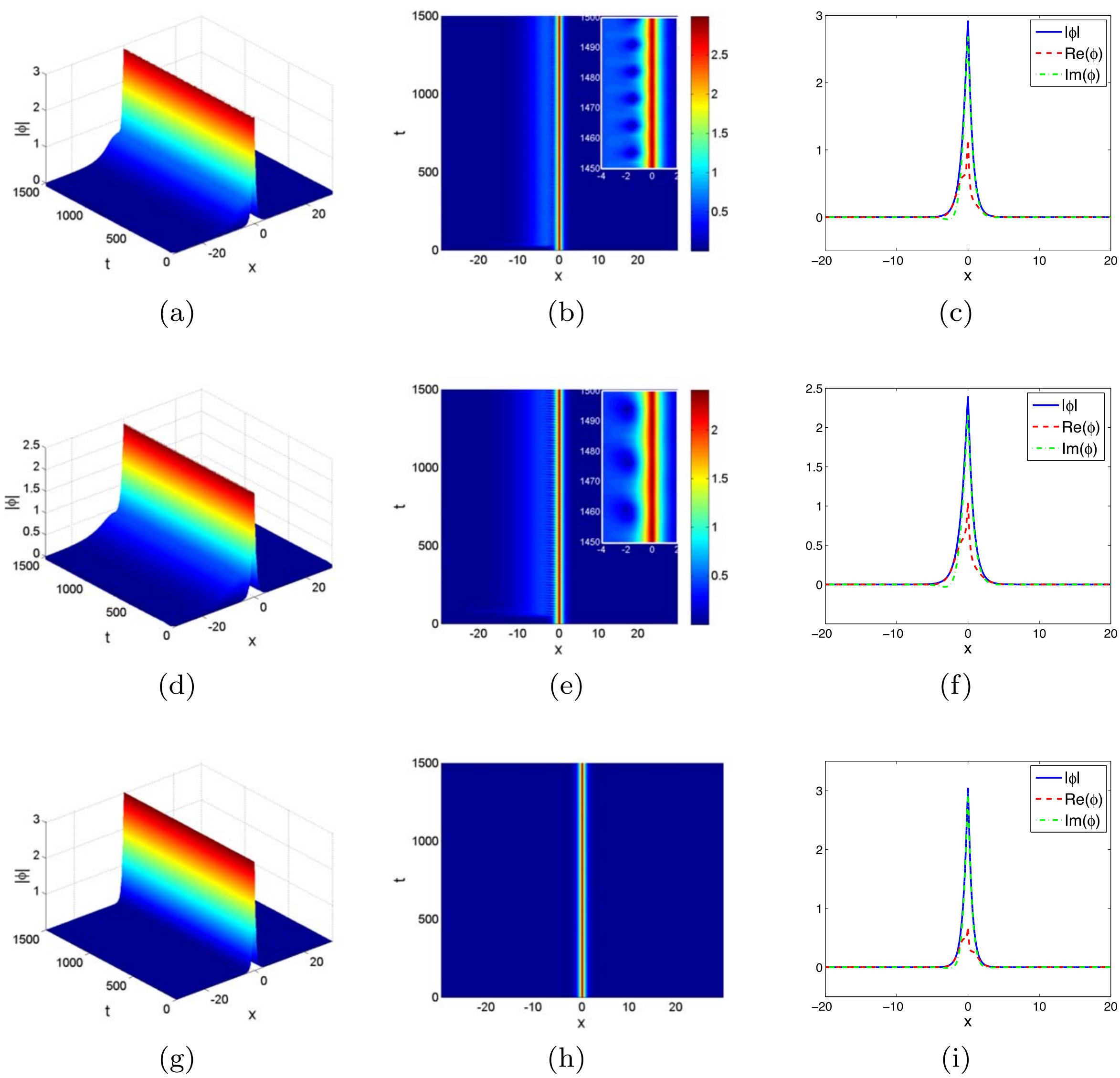

Figure 5. Stable evolution of nonlinear modes under near $\mathcal{PT}$-symmetric δ-signum potential. (a), (b), (c) $V_0 = 0.4$, $W_0 = 2$, (d), (e), (f) $V_0 = 0.4$, $W_0 = 1.5$, (g), (h), (i) $V_0 = 1$, $W_0 = 2$. Other parameters are $\alpha_1 = \beta_1 = \beta_2 = 1$, $\alpha_2 = -1$, $W_1 = 5$.

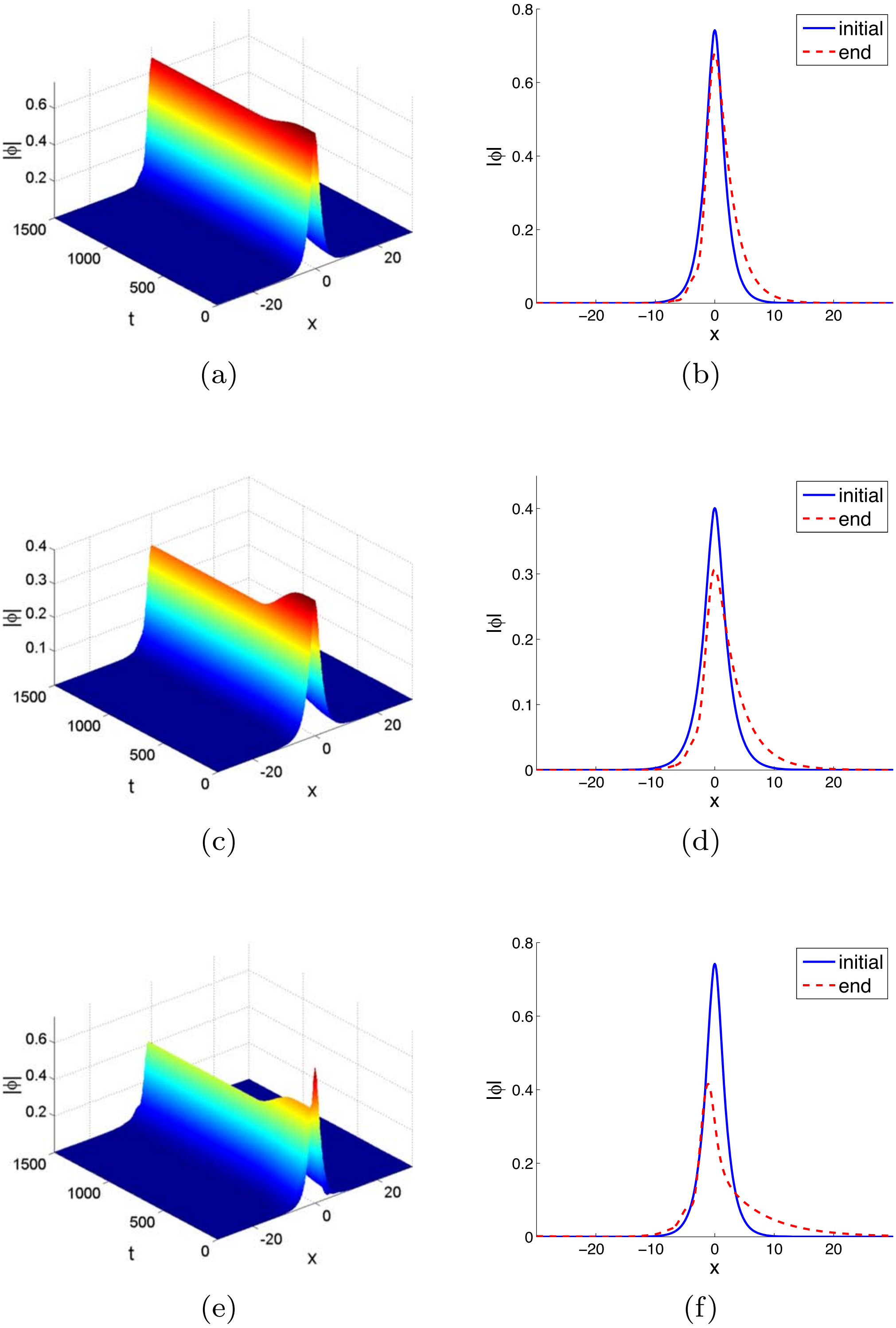

Figure 6. Adiabatic excitation and evolution of the nonlinear modes under near $\mathcal{PT}$-symmetric Scarf-II potential. (a, b) $W_0 = 0$, $W_1 = 1$, (c), (d) $W_0 = 0$, $W_1 = 0.5$, (e), (f) $W_0^{(\text{ini})} = 0$, $W_0^{(\text{end})} = 2$, $W_1^{(\text{ini})} = 1$, $W_1^{(\text{end})} = 0$ and other parameters are $\alpha_2 = -1$, $\alpha_1 = \beta_1 = \beta_2 = V_0 = 1$, $\sigma^{(\text{ini})} = \gamma^{(\text{ini})} = \rho^{(\text{ini})} = 0$, $\sigma^{(\text{end})} = \gamma^{(\text{end})} = \rho^{(\text{end})} = 1$.

The process can be divided into two stages: the excitation stage ($0 < t < 500$) and the propagation stage ($500 \leqslant t \leqslant 1500$). In the excitation stage, ξ changes constantly from $\xi^{(\text{ini})}$ to $\xi^{(\text{end})}$ and remains unchanged in the propagation stage. We generate the parameters σ, γ, ρ, V_0, W_0 and W_1 by $\xi(t)$. When $\xi^{(\text{ini})} = \xi^{(\text{end})}$, the function $\xi(t)$ turns into a constant. Figures 6(a), (c) and (e) display the stable excitation and evolution of the nonlinear modes. With σ, γ and ρ changing from 0 to 1, the amplitudes of nonlinear modes are all decreasing. Then we excite W_0 and W_1 simultaneously to meet $\mathcal{PT}$-symmetric Scarf-II potential in figure 6(e). In contrast with figure 6(a), the initial condition is the same and the final state changes greatly. In addition, the amplitude changes rapidly during the excitation stage for a short time.

4. Conclusions

In this paper, we study the higher-order GGLE, i.e. equation (1), with variable parameters and near $\mathcal{PT}$-symmetric potentials. Under some constraints, the analytical solutions of equation (1) have been derived by the Hirota bilinear method. And several structures of solitons have also been illustrated in figures by the modulation of corresponding parameters. With the near $\mathcal{PT}$-symmetric Scarf-II and δ-signum potentials introduced, stability of the nonlinear modes is proved via numerical simulations. Through the process of adiabatic excitation, stable nonlinear modes are also displayed. The results obtained might advance further investigations on generalized Ginzburg–Landau models by means of analytical and numerical methods. These new findings of nonlinear modes in the generalized Ginzburg–Landau model might be potentially applied to hydrodynamics, optics and matter waves in Bose–Einstein condensates.

Acknowledgments

We express our sincere thanks to all the members of our discussion group for their valuable comments.

Disclosures

The authors declare no conflicts of interest.

References

[1] Haus H A and Wong W S 1996 Solitons in optical communications *Rev. Mod. Phys.* **68** 423–44
[2] Skarka V and Aleksic N B 2007 Dissipative optical solitons *ACTA Phys. Pol.* A **112** 791–8
[3] Turitsyn S K, Bogdanov S and Redyuk A 2020 Soliton-sinc optical pulses *Opt. Lett.* **45** 5352
[4] Zhou Q, Luan Z, Zeng Z and Zhong Y 2022 Effective amplification of optical solitons in high power transmission systems *Nonlinear Dyn.* **109** 3083–89
[5] Zhou Q, Wang T, Biswas A and Liu W 2022 Nonlinear control of logic structure of all-optical logic devices using soliton interactions *Nonlinear Dyn.* **107** 1215–22
[6] Pelinovsky D E and Yang J K 2005 Stability analysis of embedded solitons in the generalized third-order nonlinear Schrödinger equation *Chaos* **15** 037115
[7] Zhang H P, Li B and Chen Y 2010 Some exact solutions to the inhomogeneous higher-order nonlinear Schrödinger equation by a direct method *Chin. Phys.* B **19** 060302
[8] Li J H and Li B 2021 Solving forward and inverse problems of the nonlinear Schrödinger equation with the generalized $\mathcal{PT}$-symmetric Scarf-II potential via PINN deep learning *Commun. Theor. Phys.* **73** 125001
[9] Triki H, Azzouzi F and Grelu P 2013 Multipole solitary wave solutions of the higher-order nonlinear Schrödinger equation with quintic non-Kerr terms *Opt. Commun.* **309** 71–9
[10] Zhou Q 2022 Influence of parameters of optical fibers on optical soliton interactions *Chin. Phys. Lett.* **39** 010501
[11] Zhou Q, Zhong Y, Triki H, Sun Y, Xu S, Liu W and Biswas A 2022 Chirped bright and kink solitons in nonlinear optical fibers with weak nonlocality and cubic-quantic-septic nonlinearity *Chin. Phys. Lett.* **39** 044202
[12] Zhou Q, Triki H, Xu J, Zeng Z, Liu W and Biswas A 2022 Perturbation of chirped localized waves in a dual-power law nonlinear medium *Chaos, Solitons Fractals* **160** 112198
[13] Zhou Q, Xu M, Sun Y, Zhong Y and Mirzazadeh M 2022 Generation and transformation of dark solitons, anti-dark solitons and dark double-hump solitons *Nonlinear Dyn.* (https://doi.org/10.1007/s11071-022-07673-3)
[14] Pak O S, Lam C K, Nakkeeran K, Malomed B, Chow K W and Senthilnathan K 2009 Dissipative solitons in coupled complex Ginzburg-Landau equations *J. Phys. Soc. Jpn.* **78** 084001
[15] Fan J S and Ni G X 2013 Uniform existence for a 3D time-dependent Ginzburg-Landau model in superconductivity *Appl. Math. Lett.* **26** 814–9
[16] Ignat R, Nguyen L, Slastikov V and Zarnescu A 2014 Uniqueness results for an ODE related to a generalized Ginzburg-Landau model for liquid crystals *SIAM. J. Math. Anal.* **46** 3390–425
[17] Dai Z D, Huang Y and Sun X 2010 Long-time behavior of solution for coupled Ginzburg-Landau equations describing Bose-Einstein condensates and nonlinear optical waveguides and cavities *J. Math. Anal. Appl.* **362** 125–39
[18] Yomba E and Kofane T C 2000 Solutions of the lowest order complex Ginzburg-Landau equation *J. Phys. Soc. Jpn.* **69** 1027–32
[19] Soto-Crespo J M, Akhmediev N and Ankiewicz A 2000 Pulsating, creeping, and erupting solitons in dissipative systems *Phys. Rev. Lett.* **85** 2937–40
[20] Akhmediev N, Soto-Crespo J M and Town G 2001 Pulsating solitons, chaotic solitons, period doubling, and pulse coexistence in mode-locked lasers: complex Ginzburg-Landau equation approach *Phys. Rev.* E **63** 056602
[21] Kengne E and Vaillancourt R 2009 Transmission of solitary pulse in dissipative nonlinear transmission lines *Commun. Nonlinear Sci.* **14** 3804–10
[22] Yee T L and Chow K W 2010 A 'localized pulse-moving front' pair in a system of coupled complex Ginzburg-Landau equations *J. Phys. Soc. Jpn.* **79** 124003
[23] Liu W J, Yu W T, Yang C Y, Liu M L, Zhang Y J and Lei M 2017 Analytic solutions for the generalized complex Ginzburg-Landau equation in fiber lasers *Nonlinear Dyn.* **89** 2933–9
[24] Wong P, Pang L H, Wu Y, Lei M and Liu W J 2016 Novel asymmetric representation method for solving the higher-order Ginzburg-Landau equation *Sci. Rep.* **6** 24613
[25] Li W Y, Ma G L, Yu W T, Zhang Y J, Liu M L, Yang C Y and Liu W J 2018 Soliton structures in the (1+1)-dimensional Ginzburg-Landau equation with a parity-time-symmetric potential in ultrafast optics *Chin. Phys.* B **27** 030504
[26] Huang J, Leng M M and Dai Z D 2009 Novel homoclinic and heteroclinic solutions for the 2D complex cubic Ginzburg-Landau equation *Phys. Lett.* A **374** 258–63
[27] Djob M and Kofane T C 2017 Dissipative optical bullets modeled by the cubic-quintic-septic complex Ginzburg-Landau equation with higher-order dispersions *Commun. Nonlinear Sci.* **48** 179–99
[28] Gurevich S V, Schelte C and Javaloyes J 2019 Impact of high-order effects on soliton explosions in the complex cubic-quintic Ginzburg-Landau equation *Phys. Rev.* A **99** 061803

[29] Uzunov I M and Nikolov S G 2020 Influence of the higher-order effects on the solutions of the complex cubic-quintic Ginzburg-Landau equation *J. Mod. Opt.* **67** 1–13
[30] Yuan Y Y and Liu W J 2019 Stable transmission of solitons in the complex cubic-quintic Ginzburg-Landau equation with nonlinear gain and higher-order effects *Appl. Math. Lett.* **98** 171–6
[31] He Y J and Mihalache D 2013 Lattice solitons in optical media described by the complex Ginzburg-Landau model with $\mathcal{PT}$-symmetric periodic potentials *Phys. Rev.* A **87** 013812
[32] Chen Y, Yan Z Y and Liu W J 2018 Impact of near-$\mathcal{PT}$ symmetry on exciting solitons and interactions based on a complex Ginzburg-Landau model *Opt. Express* **26** 33022–34
[33] Alaeian H and Dionne J A 2014 Parity-time-symmetric plasmonic metamaterials *Phys. Rev.* A **89** 033829
[34] Regensburger A, Bersch C, Miri M A, Onishchukov G, Christodoulides D N and Peschel U 2012 Parity-time synthetic photonic lattices *Nature* **488** 167–71
[35] Hodaei H, Miri M A, Heinrich M, Christodoulides D N and Khajavikhan M 2014 Parity-time-symmetric microring lasers *Science* **346** 975–8
[36] Guo A, Salamo G, Duchesne D, Morandotti R, Volatier-Ravat M, Aimez V, Siviloglou G and Christodoulides D 2009 Observation of $\mathcal{PT}$-symmetry breaking in complex optical potentials *Phys. Rev. Lett.* **103** 093902
[37] Ruter C E, Makris K G, El-Ganainy R, Christodoulides D N, Segev M and Kip D 2010 Observation of parity-time symmetry in optics *Nat. Phys.* **6** 192–5
[38] Regensburger A, Miri M A, Bersch C, Nager J, Onishchukov G, Christodoulides D N and Peschel U 2013 Observation of defect states in $\mathcal{PT}$-symmetric optical lattices *Phys. Rev. Lett.* **110** 223902
[39] Zhang J R, Zhang J Q, Zheng Z L, Lin D and Shen Y J 2022 Dynamic behavior and stability analysis of nonlinear modes in the fourth-order generalized Ginzburg-Landau model with near $\mathcal{PT}$-symmetric potentials *Nonlinear Dyn.* **109** 1005–17
[40] Yuan Y Y, Liu W J, Zhou Q and Biswas A 2020 Dromion-like structures and periodic wave solutions for variable-coefficients complex cubic-quintic Ginzburg-Landau equation influenced by higher-order effects and nonlinear gain *Nonlinear Dyn.* **99** 1313–19
[41] Agrawal G P 1989 *Nonlinear Fiber Optics* (New York: Academic)
[42] Chow K W, Lam C K, Nakkeeran K and Malomed B 2008 Transmission and stability of solitary pulses in complex Ginzburg-Landau equations with variable coefficients *J. Phys. Soc. Jpn.* **77** 054001
[43] Liu W J, Tian B, Jiang Y, Sun K, Wang P, Li M and Qu Q X 2011 Soliton solutions and Bäcklund transformation for the complex Ginzburg-Landau equation *Appl. Math. Comput.* **217** 4369–76
[44] Hirota R 1980 *The Direct Method in Soliton Theory* (Berlin: Springer)
[45] Yang J K 2010 *Nonlinear Waves in Integrable and Nonintegrable Systems* (Philadelphia, PA: SIAM)
[46] Chen Y, Yan Z Y and Mihalache D 2019 Stable flat-top solitons and peakons in the $\mathcal{PT}$-symmetric delta-signum potentials and nonlinear media *Chaos* **29** 083108
[47] Shen Y J, Wen Z C, Yan Z Y and Hang C 2018 Effect of $\mathcal{PT}$-symmetry on nonlinear waves for three-wave interaction models in the quadratic nonlinear media *Chaos* **28** 043104